Modeling Method of Stray Magnetic Couplings in an EMC Filter for Power Electronic Devices *

Takashi MASUZAWA   Eckart HOENE   Stefan HOFFMANN

Klaus-Dieter LANG

This paper proposes a remarkably efficient modeling method of stray magnetic couplings in an Electromagnetic Compatibility (EMC) filter that focuses on the dominant magnetic field in a power electronic device. The proposed modeling method was applied for simulating the filter performance of an EMC filter for a Silicon Carbide (SiC) solar inverter, and its effectiveness was verified through a comparison of the measurement and simulation results. With the proposed modeling method, the influence of the stray magnetic couplings on the filter performance can be predicted well. Further, the results matched those of the measurement and simulation with a conventional modeling method. Accordingly, the number of stray magnetic couplings required for accurate prediction can be dramatically reduced from 325 to just one.

Key words :
Electromagnetic compatibility, EMC filter, stray magnetic coupling, electromagnetic modeling

1. Introduction

An EMC filter plays a key role to comply with the EMC standards. On the other hand, apart from an effect of EMC suppression, an EMC filter can lead to an additional space and cost. Thus, it has to be optimally designed. To realize an optimal filter design, stray magnetic couplings between components should be properly considered in addition to the self stray impedance of the components[1][2][3]. However, it is not practical to consider all stray magnetic couplings existing in a power electronic device. Because a product designer can not determine which part of an EMC filter has to be modified for better performance by using simulation with consideration of a huge number of stray magnetic couplings. Furthermore, at an early stage of product design process, a product designer has no detailed 3D geometry of a product. Therefore a reduction of the complexity of the modeling, namely an extraction of major couplings, is needed especially in a product design process. With respect to an extraction of major couplings, the idea to identify major couplings has been suggested in[4], but however, since the idea is empirically developed using

a specific prototype, it is considerably ambiguous whether the idea is applicable to general EMC filter designs.

In this paper, a highly efficient modeling method of the stray magnetic couplings based on the simplification method [5] is proposed and applied to the filter performance simulation of the EMC filter for the SiC solar inverter [6]. A comparison between the measurement and the simulation is carried out to prove that the proposed modeling method can significantly reduce an effort to accurately predict influence of stray magnetic couplings.

2. Simplification method of modeling of stray magnetic coupling

2.1 Complexity of considering stray magnetic coupling

Fig. 1 shows an EMC filter consisting of one coil, two capacitors and stray inductances. Even in this simple filter, there are nine relevant stray inductances resulting in 36 stray magnetic couplings to be considered. The stray inductances originate from the PCB tracks, the connecting cables, the leads of components, the leakage magnetic flux from the coil, and so on. For example, the two stray inductances in the branch including the coil correspond to the PCB tracks connected to the coil and the leakage inductance of the coil respectively. The stray inductance in the branch including the capacitor is the combined stray inductance of the capacitor and the PCB tracks connected to the capacitor.
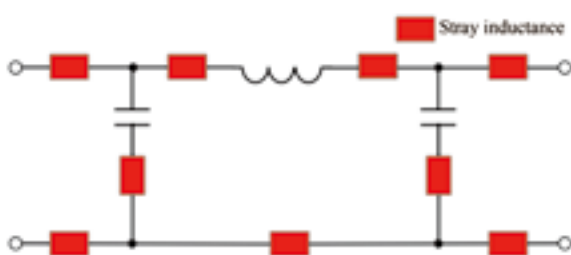

Fig. 1   EMC filter considering stray inductance

2.2 Basic idea of simplification method

The EMC filter in **Fig. 1** is assumed to be a part of the half-bridge circuit as shown in **Fig. 2**. Either of the capacitors in the EMC filter is the DC link capacitor, which is a part of the commutation cell. The noise current, the alternating current with high amplitude flowing in the commutation cell, produces a voltage drop along the DC link capacitor. And consequently, this voltage drop mainly produces a conducted noise which spreads to the power supply lines through the EMC filter.

Although most of the conducted noise directly propagates to the power supply, a considerable part of the conducted noise can also indirectly propagate via magnetic couplings. The influence of the indirect propagation will significantly increase, particularly when there is a large difference in amplitude between the conducted noise at the input and the output of the EMC filter. As a result, the filter performance of the EMC filter is severely deteriorated by the indirect propagation.
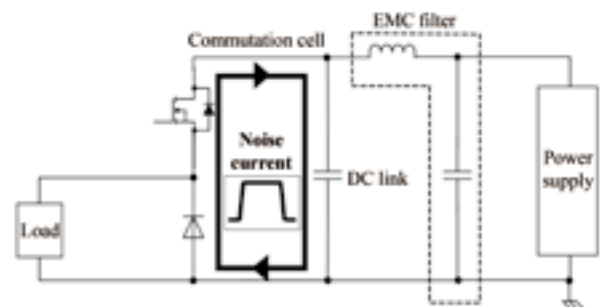

Fig. 2   Noise current in half-bridge circuit.

The simplification method we propose is based on identifying current loops with high amplitude and ones with low amplitude in the EMC filter. Current loops with high amplitude radiate strong magnetic flux which is picked up by current loops with low amplitude.

Fig. 3 illustrates the basic idea of the simplification method. The equivalent circuit of the half-bridge circuit is divided into three parts: the input loop, the high impedance area, and the output loop. The

input loop can be, for example, the commutation cell in the half-bridge circuit composed of the current source I_{in}, the impedance of the current source Z_{in}, the impedance of the input capacitor (the DC link capacitor) Z_{Cin}, and the relevant stray inductances[7]. The current I_{in} generates the large magnetic flux Φ_{in}. And the output loop can be, for example, the current loop composed of the impedance of the output capacitor Z_{Cout}, the impedance of the power supply including connectors, cables and Line Impedance Stabilization Network (LISN) Z_{out}, and the relevant stray inductances.
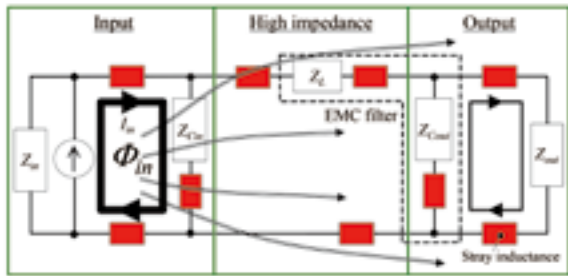

Fig. 3   Basic idea of simplification method

The magnetic flux Φ_{in} generated from the input loop can cause a significant magnetic coupling between the input loop and the output loop. And also, since the high impedance components Z_L like a filter coil connect the input loop to the output loop, the high impedance area can be sensitive to a magnetic coupling with the input loop as well. An influence of a magnetic coupling can be theoretically defined as an induced voltage. In **Fig. 4**, e_{high} and e_{out} are the induced voltages caused by the magnetic couplings in the high impedance area and the output loop respectively.
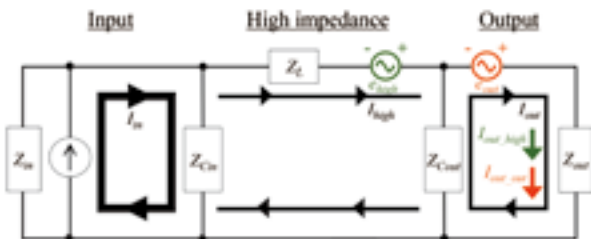

Fig. 4   Influence of magnetic coupling in EMC filter

These induced voltages e_{high} and e_{out} cause the additional currents in the output loop I_{out_high} and I_{out_out}, which deteriorate the performance of the EMC filter. I_{out_high} and I_{out_out} are given by:

$$
\begin{aligned}
I_{out\_high} &= \frac{Z_{Cout}}{Z_{Cout} + Z_{out}} I_{high} \\
&= \frac{Z_{Cout}}{Z_{Cout} + Z_{out}} \frac{e_{high}}{\dfrac{Z_{in}Z_{Cin}}{Z_{in} + Z_{Cin}} + Z_L + \dfrac{Z_{Cout}Z_{out}}{Z_{Cout} + Z_{out}}}
\end{aligned} \tag{1}
$$

$$
\begin{aligned}
I_{out\_out} &= \frac{e_{out}}{(Z_{in} /\!/ Z_{Cin} + Z_L) /\!/ Z_{Cout} + Z_{out}} \\
&= \frac{e_{out}}{\dfrac{\left(\dfrac{Z_{in}Z_{Cin}}{Z_{in} + Z_{Cin}} + Z_L\right) Z_{Cout}}{\dfrac{Z_{in}Z_{Cin}}{Z_{in} + Z_{Cin}} + Z_L + Z_{Cout}} + Z_{out}}
\end{aligned} \tag{2}
$$

I_{out_high} is the current flowing in the output loop caused by e_{high}, I_{out_out} is the current flowing in the output loop caused by e_{out}, and I_{high} is the current flowing in the high impedance area caused by e_{high}.

Since the impedance of capacitors Z_{Cin} and Z_{Cout} and the impedance of the PCB tracks Z_{in} are generally much smaller than the impedance of the high impedance component Z_L, the following approximations can be applied.

$$
\frac{Z_{in}Z_{Cin}}{Z_{in} + Z_{Cin}} + Z_L + \frac{Z_{Cout}Z_{out}}{Z_{Cout} + Z_{out}} \approx Z_L \tag{3}
$$

$$
\left(\frac{Z_{in}Z_{Cin}}{Z_{in} + Z_{Cin}} + Z_L\right) Z_{Cout} \approx Z_L Z_{Cout} \tag{4}
$$

$$
\frac{Z_{in}Z_{Cin}}{Z_{in} + Z_{Cin}} + Z_L + Z_{Cout} \approx Z_L \tag{5}
$$

With the above-mentioned approximations (3)-(5), I_{out_high} and I_{out_out} can be simplified as follows:

$$
I_{out\_high} = \frac{Z_{Cout}}{Z_{Cout} + Z_{out}} \frac{e_{high}}{Z_L} \tag{6}
$$

$$
I_{out\_out} = \frac{e_{out}}{Z_{Cout} + Z_{out}} \tag{7}
$$

The influence of e_{high} and e_{out} can be compared using a ratio between the additional currents in the output loop I_{out_high} and I_{out_out} expressed by (6) and (7). The ratio r_{Iout} is described as:

$$r_{Iout} = \left| \frac{I_{out\_high}}{I_{out\_out}} \right| = \left| \frac{Z_{Cout}}{Z_L} \right| \left| \frac{e_{high}}{e_{out}} \right| \quad \cdots\cdots\cdots\cdots\cdots\cdots\cdots\cdots (8)$$

Unless e_{high} is exceptionally larger than e_{out}, the ratio r_{Iout} is basically much smaller than 1, because Z_L is much larger than Z_{Cout} from the viewpoint of a filter design; otherwise the EMC filter has no effect on noise attenuation. Based on this premise, the stray magnetic couplings in the EMC filter can be simplified as described in **Fig. 5**, where $M_{in\text{-}out}$ is the major stray magnetic coupling between the input loop and the output loop.
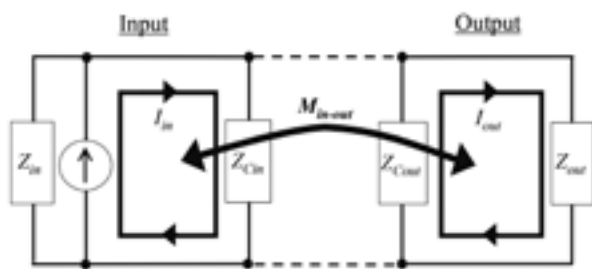

Fig. 5   IMajor stray magnetic coupling in EMC filter

3. Application of proposed modeling method

In this chapter, to clarify its applicability and its problems to be solved for application to actual products, we apply the proposed modeling method to an EMC filter for a SiC solar inverter.

3.1 Tested EMC filter

Fig. 6 depicts the EMC filter for the SiC solar inverter used in the verification.
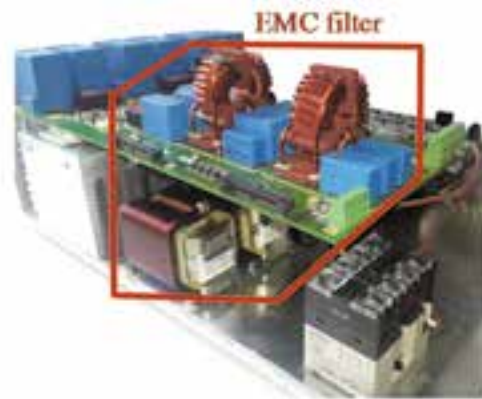

Fig. 6   Tested EMC filter for SiC solar inverter

Fig. 7 shows the circuit schematic of the tested EMC filter used for the three-phase grid connection. The filter is composed of the three output inductors L_{out}, the two common mode choke coils L_{CM}, the nine X-capacitors C_X, and the two Y-capacitors C_Y. This EMC filter has 26 stray inductances resulting in 325 stray magnetic couplings.
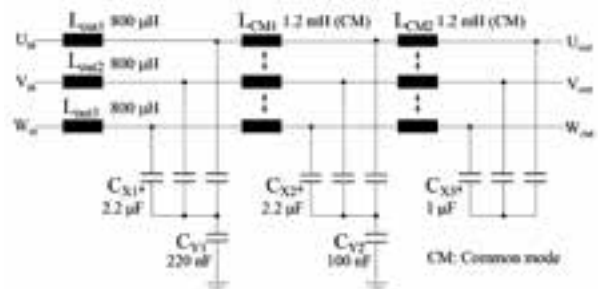

Fig. 7   Circuit schematic of the tested EMC filter

3.2 Modeling of filter capacitor

Stray magnetic couplings used in a filter performance simulation can be obtained from geometry by means of commercial 3D simulation software[8]. Furthermore, effective modeling methods of the relevant components for the 3D simulation have been reported in the past investigations[9)10)]. According to the investigations, geometry of PCB tracks and filter coils can be directly applied to the 3D simulation in most of cases.

Whereas, geometry of a filter capacitor requires a major modification, since the inner structure of

the filter capacitor is too complicated to be directly applied to the 3D simulation, as described in Fig. 8. Therefore, to obtain stray magnetic couplings, the modified capacitor model with the simplified inner structure described in Fig. 9 is applied to the 3D simulation.
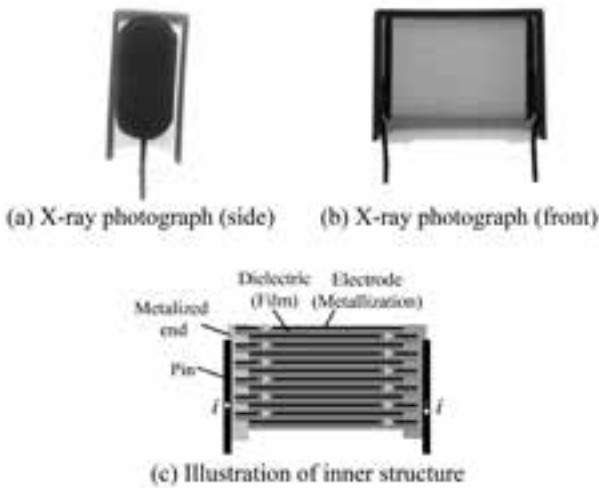

(a) X-ray photograph (side)   (b) X-ray photograph (front)

(c) Illustration of inner structure

Fig. 8   Inner structure of filter capacitor

Fig. 9   Simplified model of filter capacitor

3.3 Consideration of magnetic material

Since partial impedance is needed for the filter performance simulation of the tested EMC filter, we use the Partial Element Equivalent Circuit (PEEC) method software FastHenry[11].

To estimate an accurate stray magnetic coupling by using simulation, influences of permeability of the magnetic core should be properly considered. However, most of the commercial software including the PEEC software does not consider permeability; simulations considering permeability can lead to a tremendous increase of computational time, even if it

is possible with specific software. Thus, in simulation, we have to consider permeability of a core in a simple way only where necessary.

In [12)13], it is concluded that leakage magnetic flux from a typical common mode choke coil generated by differential mode current is nearly equal to that from a solenoid coil. That is because the magnetic fluxes inside the core, generated by the currents in both of the windings, repel each other and flow outside of the core as shown in Fig. 10. Fig. 11 illustrates the idea of the approximation. The winding of the coil can be described as the solenoid coil with the same effective magnetic length l and the same cross section A, where l is given by:

$$l = 2\pi r \frac{\theta}{360°} \quad \cdots\cdots\cdots\cdots\cdots (9)$$

Where θ is the winding coverage angle and r is the radius of the coil.
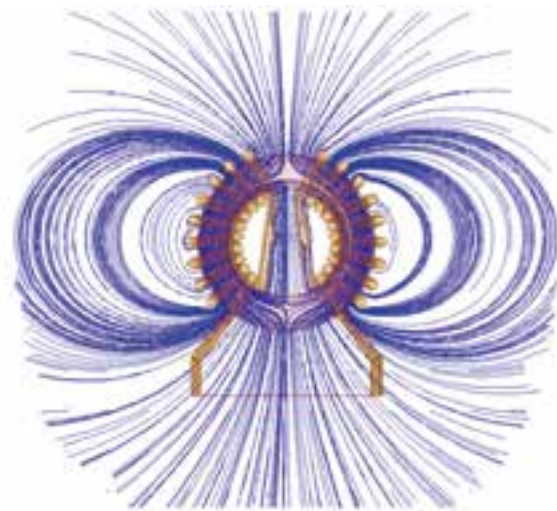

Fig. 10   Magnetic flux line by differential current
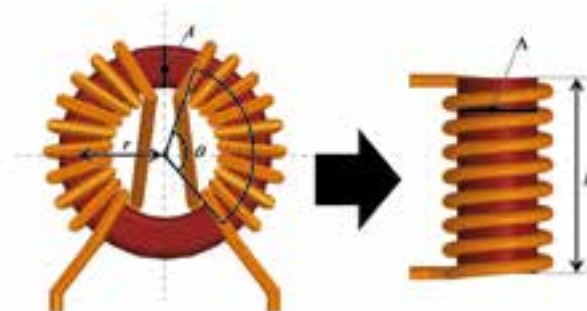

Fig. 11   Idea of approximation of leakage inductance

Based on the approximation, the effective permeability μ_{eff} related to the leakage magnetic flux from the coil is described as follows:

$$\mu_{eff} = 2.5\left(\sqrt{\frac{\pi}{A}}\frac{l}{2}\right)^{1.25} \quad\cdots\cdots\cdots\cdots\cdots\cdots\cdots\cdots (10)$$

Whereas it is assumed that the leakage magnetic flux from the coil generated by common mode current is not significantly influenced by the core, because the magnetic fluxes inside the core do not repel each other. Similarly to the common mode choke coil, it is also assumed that the leakage magnetic flux from the output inductor is not significantly influenced by the core for the same reason.

To validate the assumption, a distribution of magnetic flux from the output inductor is compared between ones with and without the core by means of 3D Finite Element Method (FEM) simulation software ANSYS HFSS[14].

The output inductor is built using a Hitachi Metals AMCC-40 core with an air gap of 1.1mm. The number of turns of the winding is 48. The horizontal and vertical wire sizes of the winding are 6mm and 2mm respectively. Fig. 12 shows the simulation model. The input current is 1A, and the simulating frequency is 1MHz.
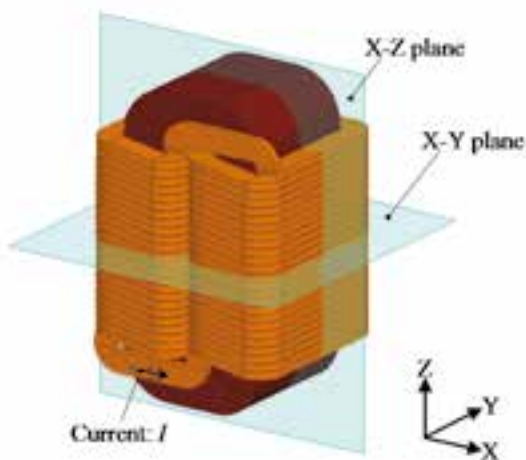

Fig. 12　Model for simulation of magnetic flux distribution

Fig. 13 presents the comparison of the simulated magnetic flux distribution on X-Y and X-Z planes between the output inductors with and without the core.
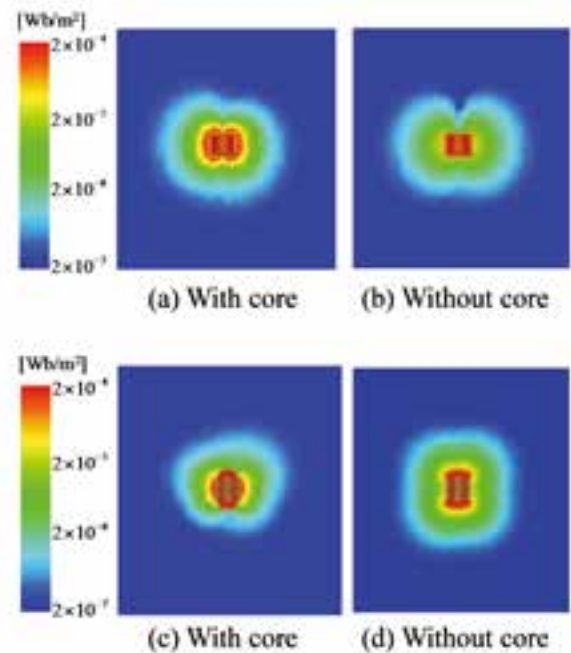

Fig. 13　Distribution of magnetic flux: X-Y plane in (a) and (b); X-Z plane in (c) and (d)

In Fig. 13, there is no significant difference in the distribution of the magnetic flux between the simulation results with the core and without the core. Moreover the common mode choke coil is not the main part of the output loop. Thus we reach a conclusion that it is not necessary to consider μ_{eff} of the output inductor and the common mode choke coils for the filter performance simulation conducted in the next chapter. On the other hand, it is highly likely that μ_{eff} needs to be considered by using the above mentioned approximation for the simulation in differential mode. In future work, the influence of μ_{eff} needs to be investigated in more detail.

3.4 Applicability to the tested EMC filter

As stated in the preceding chapter, a major stray magnetic coupling basically occurs between an input loop and an output loop in an EMC filter. In this section, the applicability of the proposed modeling

ECU

method to the tested EMC filter is verified.

In **Fig. 4**, the induced voltage in the output loop e_{out} is generated by the stray magnetic coupling between the input loop and the output loop M_{in-out}. And similarly to e_{out}, the induced voltage in the high impedance area e_{high} is dominantly generated by the stray magnetic coupling between the input loop and the filter coil M_{in-L}. Hence e_{out} and e_{high} can be described as follows:

$$e_{out} = M_{in-out} \frac{dI_{in}}{dt} \quad\cdots\cdots\cdots\cdots\cdots\cdots\cdots\cdots\cdots\cdots (11)$$

$$e_{high} \approx M_{in-L} \frac{dI_{in}}{dt} \quad\cdots\cdots\cdots\cdots\cdots\cdots\cdots\cdots\cdots (12)$$

By using (11) and (12), the ratio of the output current r_{Iout} is given by:

$$r_{Iout} = \left| \frac{I_{out\_high}}{I_{out\_out}} \right| = \left| \frac{Z_{Cout}}{Z_L} \right| \left| \frac{e_{high}}{e_{out}} \right| = \left| \frac{Z_{Cout}}{Z_L} \right| \frac{M_{in-L}}{M_{in-out}} \quad\cdots (13)$$

Fig. 14 presents calculated r_{Iout} using (13), where the simulated values of M_{in-out} and M_{in-L} are 3.2nH and 0.25nH respectively.
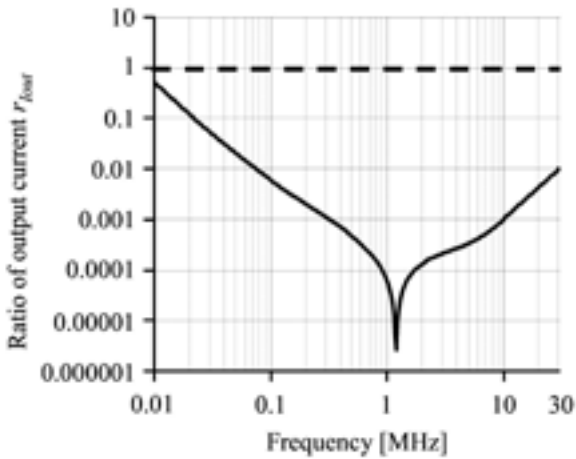

Fig. 14   Calculated ratio of output current r_{Iout}.

It can be seen that calculated r_{Iout} is smaller than 0.1 in the frequency range from 0.02MHz to 30MHz. Therefore it is concluded that the influence of the induced voltage in the high impedance area e_{high} is negligible in this frequency range. This fact in **Fig. 14** corroborates that the major stray magnetic coupling in the tested EMC filter is M_{in-out}.

4. Comparison of filter performance

To verify the effectiveness of the proposed modeling method, the filter performance of the EMC filter is compared between a measurement and a simulation. **Fig. 15** depicts a system configuration for a measurement of a filter performance P_f in common mode. In this measurement, P_f is defined as the ratio of the output voltage A to the reference voltage *Ref*, measured by means of a Gain-Phase analyzer: Agilent 4395A. The range of measuring frequency is set from 0.01MHz to 30MHz. The nanocrystalline cores in **Fig. 15** are used to suppress common mode current flowing through the Gain-Phase analyzer.
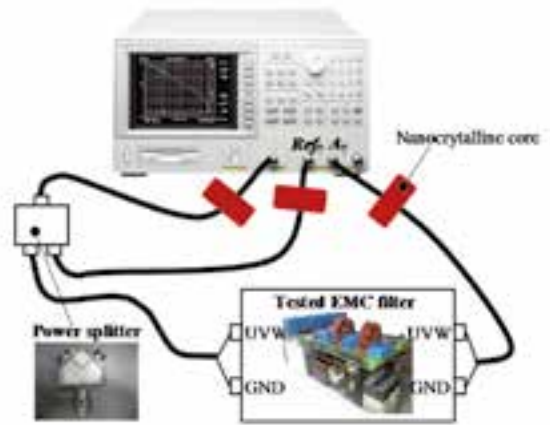

Fig. 15   System configuration for measurement of P_f

Fig. 16 shows the circuit simulation model with the highlighted input loop, output loop, and major stray magnetic coupling M_{in-out}. The software used for the circuit simulation is Portunus[15].
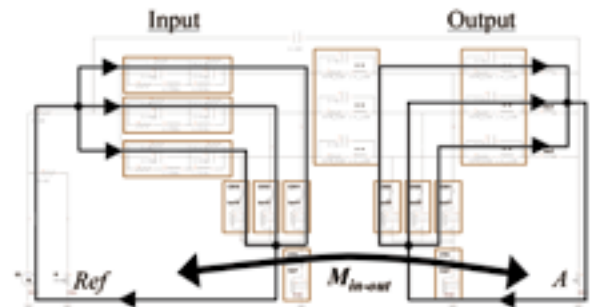

Fig. 16   Circuit simulation model with the highlighted input loop, output loop, and major stray magnetic coupling

The major stray magnetic coupling incorporated into the circuit simulation model described in **Fig. 16** is obtained from the 3D geometry by using the PEEC method software. **Fig. 17** depicts the 3D simulation model including the output inductor, the common mode choke coil, the X and Y-capacitors, the connecting wires and the PCB tracks. The inductor and the coil have no core based on the conclusion in the preceding chapter.
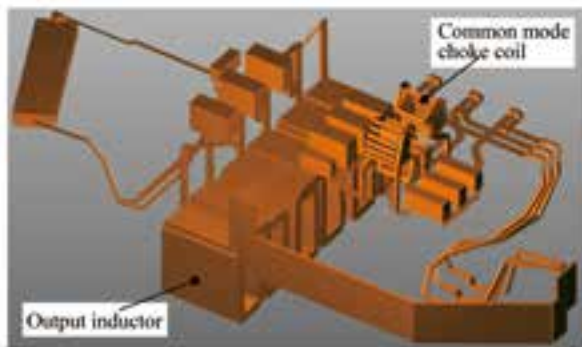

Fig. 17   Simulation model of tested EMC filter

Fig. 18 shows a comparison of the filter performance P_f in common mode between the measurement and the simulation with the following three conditions: considering the classical stray impedances (ESR and ESL of a capacitor and EPR and EPC of a coil), considering the classical stray impedances and all the stray magnetic couplings (325 couplings), considering the classical stray impedances and only the major stray magnetic couplings (1 coupling) derived with the proposed modeling method. Where ESR is an equivalent series resistance, ESL is an equivalent series inductance, EPR is an equivalent parallel resistance, and EPC is an equivalent parallel capacitance.
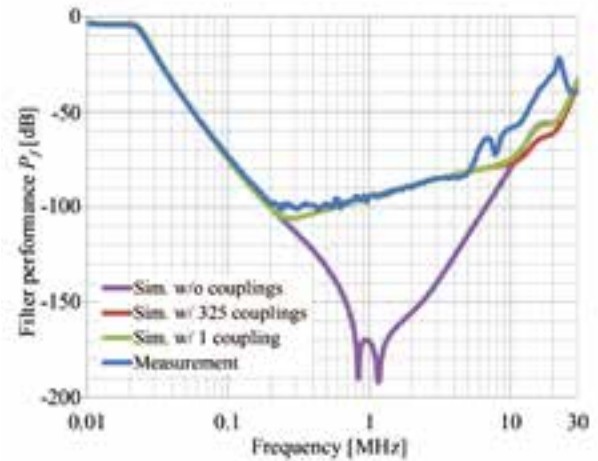

Fig. 18   Comparison of P_f between simulation and measurement

In **Fig. 18**, the measurement result and the simulation results considering all the couplings and only the major coupling show a good agreement in the frequency range up to 10MHz. On the other hand, the simulation without consideration of the stray magnetic coupling inaccurately predicts the filter performance with the difference of more than 100dB compared to the measurement result. Most importantly, the simulation using the proposed modeling method realizes a comparably accurate prediction in comparison with the simulation using the conventional modeling method, even though the number of the considered stray magnetic couplings is dramatically reduced from 325 to just one. Regarding the difference in the frequency range higher than 10MHz, it is assumed that it is caused by the following three elements: 1) the connections between the shielded cables and the tested EMC filter forming a small loop, which can be affected by magnetic flux, 2) the residual common mode current flowing through the measuring instrument, and 3) the changed distribution of magnetic flux of the coils due to the stray capacitances over their self resonance frequencies [16].

5. Conclusion

In this paper, the highly efficient modeling method of stray magnetic couplings based on the simplification method was proposed. And its effectiveness was verified by comparing the performance of the EMC filter for the SiC solar inverter, between the measurement and the simulation. Moreover, the simple approximation to consider permeability of a core and its necessity in differential mode and common mode were also outlined. The results of the comparison showed that the proposed modeling method could significantly reduce the number of stray magnetic couplings considered for an accurate simulation.

References

1) E. Hoene, A. Lissner, S. Weber, S. Guttowski, W. John, and H. Reichl, "Simulating Electromagnetic Interactions in High Power Density Converters," in Proc. IEEE 36th Power Electron. Spec. Conf., pp.1665-1670, 2005.

2) T. De Oliveira, J. Guichon, J. Schanen, and L. Gerbaud, "PEEC-Models for EMC filter layout optimization," in Integrated Power Electronics Systems (CIPS), paper 13.3, 2010.

3) I. Kovacevic, A. Muesing, T. Friedli, and J. W. Kolar, "Electromagnetic modeling of EMI input filters," in Integrated Power Electronics Systems (CIPS), paper 02.1, 2012.

4) S. Wang, F.C. Lee, D. Chen, and W. G. Odendaal, "Effects of Parasitic Parameters on EMI Filter Performance," IEEE Trans. Power Electron., vol.19, no.3, pp.869-877, 2004.

5) T. Masuzawa, and E. Hoene, "A simplification of a modeling of stray magnetic couplings in EMC filters," in PCIM Europe 2013, pp. 779-786, 2013.

6) S. Hoffmann, E. Hoene, and O. Zeiter, "Electrical, thermal and electromagnetic design of a SiC solar inverter: a case study," in PCIM Europe 2013, pp. 470-477, 2013.

7) Z. Yu-lin, and Z. Zheng-ming, "Comparison of Parasitic Parameters Extraction methods and Equivalent Circuits for a Ground Model, Electrical Machines and Systems," in ICEMS 2008, pp.3781-3784, 2008.

8) S. Weber, E. Hoene, S. Guttowski, W. John, and H. Reichl, "On coupling with EMI capacitors," in IEEE Symposium on EMC (EMC), pp.336-341, 2004.

9) T. De Oliveira, J. Schanen, J. Guichon, and L. Gerbaud, "Optimal stray magnetic couplings for EMC filters," IEEE Trans. Ind. Appl., vol.49, no.4, pp.1619-1627, 2013.

10) E. Hoene, W. John and H. Reichl, "Simulation of Conducted Electromagnetic Interference of Inverter-Fed Induction Motor," in Proc. EPE'99, 1999.

11) M. Kamon, M.J. Tsuk, and J.K. White, "FASTHENRY: a multipole-accelerated 3-D inductance extraction program," IEEE Trans. Microw. Theory Tech., vol. 42, no. 9, pp. 1750-1758, 1994.

12) M. Nave, Power Line Filter Design for Switched-Mode Power Supplies. New York, NY, USA, Springer, 1991.

13) S. Weber, "Effizienter Entwurf von EMV-Filtern für leistungselektronische Geräte unter Anwendung der Methode der partiellen Elemente," Ph.D. dissertation at Technical University of Berlin, 2007.

14) ANSYS HFSS, 2014. [Online]. Available: http://www.ansys.com/

15) Portunus, 2014. [Online]. Available: http://www.adapted-solutions.com/

16) R. Wang, H. Blanchette, M. Mu, D. Boroyevich, and P. Mattavelli, "Influence of high-frequency near-field coupling between magnetic components on EMI filter design," IEEE Trans. Power Electron., vol.28, no.10, pp.4568-4579, 2013.

著者

増澤 高志
ますざわ　たかし

Eco Mobility システム開発部
SiC インバータ関連の要素技術開発に従事

Stefan Hoffmann
ステファン　ホフマン

フラウンホーファー IZM（信頼性・マイクロ
インテグレーション研究所）
パワーエレクトロニクス機器の EMC 関連
の技術開発に従事

Eckart Hoene
エッカート　ホエネ

フラウンホーファー IZM（信頼性・マイクロ
インテグレーション研究所）グループリー
ダー　オールボー大学　名誉教授
パワーエレクトロニクス機器のパッケージ
ング，システムおよび EMC 関連の技術開
発に従事

Klaus-Dieter Lang
クラウスーディーター　ラング

フラウンホーファー IZM（信頼性・マイクロ
インテグレーション研究所）所長
ベルリン工科大学　教授
ベルリン工科大学にてナノインターコネクト
関連の技術開発に従事

ECU